Scilight

Physical Models and Application
https://www.sciltp.com/journals/pma



Article

The Chimera States of a Mixed-Coupled Photosensitive Neural Networks under Time Delay

Xinlei An * and Xinyue Wang

School of Mathematics and Physics, Lanzhou Jiaotong University, Lanzhou 730070, China
* Correspondence: anxin1983@163.com

How To Cite: An, X.; Wang, X. The Chimera States of a Mixed-Coupled Photosensitive Neural Networks under Time Delay. *Physical Models and Application* **2026**, *1*(1), 3.

Received: 10 August 2026
Revised: 5 October 2026
Accepted: 29 October 2026
Published: 10 November 2026

Abstract: Information transmission delay is an inherent feature of neural networks and can significantly influence their collective dynamics. However, most previous studies on Chimera states in photosensitive neural networks have focused exclusively on electrical synaptic coupling, while the role of chemical synapses in shaping Chimera dynamics remains largely unexplored. To better mimic the complex synaptic connections in the brain, we construct a single-layer photosensitive neural network with mixed electrical and chemical synaptic coupling. We systematically investigate the effects of coupling strength and time delay on the emergence and evolution of Chimera states under three different autapse conditions: no autapse, positive-gain autapse, and negative-gain autapse. The results show that, in networks without autapses or with positive-gain autapses, Chimera states emerge primarily at relatively small time delays and are strongly influenced by the coupling strength. In contrast, in networks with negative-gain autapses, Chimera states can still be induced at relatively large time delays, while the influence of coupling strength on the collective dynamics is significantly reduced. These results demonstrate that, even after the introduction of chemical synapses into photosensitive neural networks, Chimera states remain sensitive to time delay and coupling strength. Our findings provide a new perspective for understanding the collective dynamics of neural networks with hybrid electrical and chemical synaptic coupling.

Keywords: neural networks; photosensitive neuron; chimera state; autapse; time delay

1. Introduction

Biological neural network is one of the most common complex networks in nature, and has received extensive attention in many fields in recent years. Studies have shown that the rich collective dynamic behaviors and different discharge modes in neuronal networks are closely related to various functions of organs [1,2]. Synchronization is a common phenomenon in neural networks, which can affect the brain's learning and memory functions under multi-synaptic connections [3–6]. In addition to synchronization, healthy brains also spontaneously produce non-synchronous behaviors, but abnormal non-synchronization is associated with brain diseases such as Down syndrome [7]. Clinical trials have found that synchronous and asynchronous brain phenomena can coexist in the same neuronal circuit, such as the first-night effect in humans and hemispheric sleep in birds [8], Jacimovic and Crnkic [9] named this phenomenon as Chimera state [10–15]. The Chimera state can be used as a compromise to adjust the contradiction between the coding ability of neurons and the synchronization behavior. Rybalova et al. [13] found that the size of noise and initial value can affect the existence region of Chimera state in the ring network. Remi et al. [14] induced the Chimera state by changing the size of power law index in the ring HR neural network coupled by the average field. Andrzejak et al. [15] proved that the intensity of interlayer coupling can change the

Copyright: © 2026 by the authors. This is an open access article under the terms and conditions of the Creative Commons Attribution (CC BY) license (https://creativecommons.org/licenses/by/4.0/).
Publisher's Note: Scilight stays neutral with regard to jurisdictional claims in published maps and institutional affiliations.

collective dynamics of multi-layer neural networks. Therefore, the existence range of Chimera states in neural network is related to parameters.

There are hundreds of billions of neurons in the brain, which are connected in different ways through different types of synapses [16,17]. Electrical synapses are present in various regions of the brain, such as the olivary nucleus, locus coeruleus, hypothalamus, and spinal cord. They transmit electrical signals directly through gap junction proteins and are characterized by rapid, bidirectional transmission. Chemical synapses are widely distributed throughout various regions of the cerebral cortex, hippocampus, and olfactory bulb. They transmit signals through the release and reception of neurotransmitters and are characterized by unidirectional transmission and strong plasticity. In recent years, some studies have found that a large number of electrical and chemical synapses coexist in the brains of mammals, mainly in the retina, neocortex, and spinal cord [18]. The existence of mixed coupling enables neural networks to take advantage of both electrical and chemical synapses, thereby facilitating more complex information processing and transmission. Signal transmission may be terminated or blocked when a neuronal axon is injured, such as in cases of ion channel poisoning or localized axonal stress. Under such conditions, neurons may form new synaptic connections between their own axons and dendrites, a phenomenon known as autapses. Liu et al. [19] proposed a new kind of variant spiking neural P system system with anti-spikes and autapses, which can generate/accept Turing-computable numbers with reduced use of rules or neurons. Another characteristic of neural networks is their limited information-processing capacity and signal transmission speed. Therefore, each neuron in the network experiences a different time delay during information transmission. Studies have shown that time delay affects the collective dynamics of neurons to some extent and can effectively induce neurons to tend toward synchronization, Vijayan et al. [20] investigated the impact of delay on synchronization patterns in a duplex neuronal network composed of memristive Rulkov neuronal models, the results have potential implications for understanding temporal disruptions in neuronal networks. Shavikloo et al. [21] addressed the question that how changes in the strength of the synaptic connections and transmission delays between neurons impact synchronization in a two-neuron system with multiple synapses. Zou et al. [22] proposed offline and online supervised learning algorithms for synaptic weights and delays of spiking neurons with multiple synaptic connections. In addition, Huang et al. [23] constructed a ring neural network using FitzHugh-Nagumo neuron model and researched the effects of time delay and coupling strength on the firing frequency of neurons, Hou et al. [24] introduced a time delay in transcription and translation of *Mdm2* gene expression into the network and investigated the effects on oscillation dynamics through stability and bifurcation analyses, Dong et al. [25] studied the problem of fixed-time synchronization control for memristive neural networks with discrete time delay and inertia term. Moreover, the network will appear instantaneous or permanent Chimera states when the value of time delay tends to a certain critical value.

Biological neurons remain sensitive to external stimuli and can trigger appropriate discharge patterns to respond effectively to external chemical and physical signals [26,27]. For instance, auditory neurons can convert vibration signals into electrical signals, thermosensitive neurons can convert temperature signals into electrical signals, and neurons in photosensitive neural models are sensitive to light signals. Classic neuronal circuits, such as memristor [28], Josephson junction [29], piezoelectric ceramic [30], phototube [31], thermistor [32], can be embedded with special functional devices to construct functional neuronal circuits to perceive special physical signals from the outside world. Therefore, conducting research on the functional enhancement of neurons and the dynamics of neural networks is of great theoretical significance. In recent years, scholars have conducted in-depth studies on the collective dynamics of brain neural networks, including neuronal firing patterns and the stability of synchronization phenomena within the network [33–35]. Yang et al. [36] established a star network by using electrical synaptic coupling of four photosensitive neurons and studied the synchronization phenomenon and energy balance of the network. Han et al. [37] proposed an interpretable neural network with a synchronization mechanism, the study found that the coexistence of synchronization and desynchronization occurred in this neural network, that is the Chimera state. Huang et al. [38] studied the phenomena of synchronization and Chimera states in two unidirectional coupled small-world networks by adjusting the intensity of electromagnetic induction. Rybalova et al. [39] observed that different impulse exposures could stimulate the traveling Chimera states of FHN neural network. The relevant research results of Chimera states have enabled people to generate further profound understanding of pathogenic principles of some brain diseases, it was argued that early changes in network activity are not necessarily governed by the aim of preserving long term functionality, but rather by the attempt to achieve a state that is temporarily stable [40], and paper [41] found that the emergence of distinct sets of multistable Chimera states in addition to Chimera death and synchronized states in a smallest population of three globally coupled oscillators with mean-field diffusive coupling. Paper [42] found the appearance of alternating Chimera states and transient Chimera states whenever the intralayer coupling is nonlocal and local, respectively, and paper [43] constructed a coupled nonlinear oscillator system with a topology of the modular complex network to simulate the

left and right hemispheres of the brain. Obviously, various neural networks composed of different types of functional neurons can more realistically represent the cooperation and signal interactions among different functional areas. However, investigations of Chimera states in functional neurons and neural networks remain relatively unexplored.

Based on the above discussion, this paper establishes a photosensitive neural network model with mixed coupling. The coupling strength and time delay between neurons are varied under three different conditions: no autapse, positive-gain autapse, and negative-gain autapse. The existence range and variation trends of Chimera states under different conditions are investigated. In addition, two global parameters are introduced to further characterize the collective dynamics of the neural networks. The structure of other sections is as follows: In Section 2, the photosensitive neuron model, as well as a mixed-coupling ring neuron network model are introduced. The effects of coupling intensity and time delay on dynamics behavior of the neural network are discussed in Section 3. Conclusions are given in Section 4.

2. Mathematical Model

Ma [26] suggest that the human eye can generate neural activity when it receives light. From a physical point of view, the retina performs photoelectric conversion, whereby electromagnetic energy is converted into bioelectrical signals, which then stimulate the visual functional areas of the brain in the form of action potentials and generate a response. Therefore, a photosensitive neuron model is constructed based on the FHN neuron model to describe the photoelectric effect, described as

$$\begin{cases} \dot{x} = x(1-\xi) - \dfrac{1}{3}x^3 - y + \xi u_s \\ \dot{y} = c(x - by + a - u_g) \end{cases} \tag{1}$$

where x is membrane potential, y is the slow current corresponding to the recovery variable, $u_s = B_1 \cos \omega t$ is external excitation source, $u_g = B_2 \cos \omega t$ is the expression of the output of phototube. The dimensionless parameters a, b, c, ξ are obtained from the circuit equations via the following scaling transformations:

$$\begin{cases} x = \dfrac{V_C}{V_0}, y = \dfrac{\rho i_L}{V_0}, \tau = \dfrac{t}{\rho C}, a = \dfrac{E}{V_0}, b = \dfrac{R}{\rho}, \\ \omega = \dfrac{\omega'}{\rho C}, c = \dfrac{\rho^2 C}{L}, \xi = \dfrac{\rho}{R_S}, u_s = \dfrac{V_S}{V_0}, u_g = \dfrac{V_g}{V_0}, \end{cases} \tag{2}$$

The parameter $\xi = \dfrac{\rho}{R_S}$ is a dimensionless conductance ratio, where ρ is the membrane resistance and R_S is the equivalent resistance of the phototube branch. $a = \dfrac{E}{V_0}$ represents the bias voltage from the constant voltage source in series with the phototube; $b = \dfrac{R}{\rho}$ is the ratio of the circuit resistance to the membrane resistance, controlling the recovery dynamics; and $c = \dfrac{\rho^2 C}{L}$ is the time-scale ratio between the fast membrane potential and the slow recovery variable [44].

Based on the photosensitive neuron model, a mixed-coupling ring neuron network model with 100 neurons is constructed, the specific equation is

$$\begin{cases} \dot{x}_i = x_i(1-\xi) - \dfrac{1}{3}x_i^3 - y_i + \xi u_s + I_i^{\text{aut}} + I_i^{\text{syn}} \\ \dot{y}_i = c(x_i - by_i + a - u_g) \end{cases} \tag{3}$$

where I_i^{aut} represents the electrical impulses generated on the neuron membrane due to time delay, which is used to simulate the autapse phenomenon. The autapse current is

$$I_i^{\text{aut}} = g[x_i(t-\tau) - x_i(t)] \tag{4}$$

where g is feedback gain of synapse, and τ is time delay. Autapse is defined as the difference in the membrane potential of a neuron at different times. I_i^{syn} represents mixed total synaptic current of the i neuron. In Figure 1, the i th neuron is electrically coupled to the neurons from the $i-p$ th to the $i+p$ th (excluding itself), while on one side it forms chemical synapses connection with the neurons from the $i-p-r$ th to the $i-p-1$ th, and on the other side it forms chemical synapses connection with the neurons from the $i+p+1$ th to the $i+p+r$ th, thus the mixed total synaptic current can be obtained as

$$I_i^{\text{syn}}=d\sum_{j=i-p}^{i+p}(x_j(t-\tau)-x_i(t))+d\sum_{j=i-p-r,j\neq i-p}^{j=i+p+r,j\neq i+p}-\frac{x_i(t)-V_{\text{syn}}}{1+\exp[-\lambda(x_j(t-\tau)-\theta)]} \tag{5}$$

where V_{syn} is reversal potential in the synapse, λ is ratio parameter and θ is synaptic threshold.

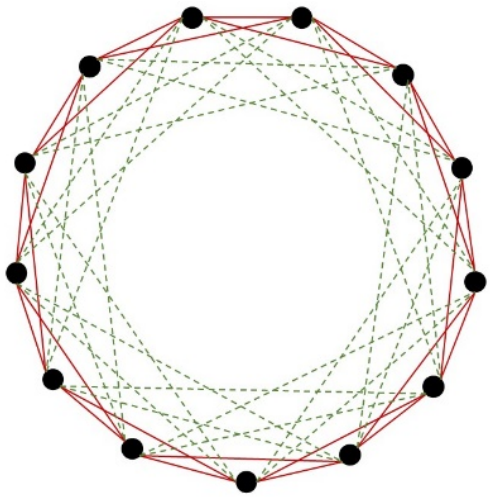


Figure 1. The ring neural network with hybrid coupling (The solid red lines represent electrical synapses and the dashed green lines represent chemical synapses).

In order to distinguish the asynchronous state, Chimera state and synchronous state in neural networks, a new parameter k_{SI} calculated by local standard deviation is introduced [44], which is called as strength of incoherence. It is essential to calculate the potential difference between adjacent neurons in the network as $w_i=x_i-x_{i-1}$, $i=1,2,\cdots,N$, and divide the neurons into three disjoint groups, the local standard deviation is defined as

$$\sigma(m)=\left\langle\sqrt{\sum_{j=n(m-1)+1}^{nm}(w_j-\langle w\rangle)^2}\right\rangle_t \tag{6}$$

where $m=1,\cdots,M$, $\langle w\rangle=\frac{1}{N}\sum_{i=1}^{N}w_i$, and $\langle\cdots\rangle_t$ represents the average value of a variable over specified time period. Calculate corresponding local standard deviation $\sigma(m)$, and k_{SI} can be expressed as

$$k_{\text{SI}}=1-\frac{\sum_{m=1}^{M}s_m}{M},\quad s_m=\Theta(\delta-\sigma(m)) \tag{7}$$

herein Θ is Heaviside step function, δ represents critical value, let δ=0.15, $n=4$. Set $s_m=1$ for the neurons of each group, that is $k_{\text{SI}}=0$ and the network is in the synchronous state when $\delta>\sigma(m), m=1,2,\cdots,M$, or the network exhibits nonsynchronous state when $k_{\text{SI}}=1$ under the condition of $\sigma(m)>\delta$. Obviously, the network presents Chimera state when $0<k_{\text{SI}}<1$. In order to further distinguish the types of Chimera states, a

parameter k_{DM} (Discontinuity Measure) is introduced to distinguish single Chimera states from the multi-cluster ones, as

$$k_{\mathrm{DM}} = \frac{\sum_{i=1}^{M} s_{i+1} - s_i}{2}, \quad s_{M+1} = s_1 \tag{8}$$

When $k_{\mathrm{DM}} = 1$, the neural network is in a single Chimera state, whereas presents the phenomenon of multiple cluster Chimera states when k_{DM} is an integer greater than 1 and in the range of $[2, \frac{M}{2}]$.

3. Numerical Simulation

In this section, the fourth-order Runge-Kutta method will be used for numerical simulation in MATLAB2018, and the fixed parameters in the neuron model are $a = 0.7$, $b = 0.8$, $c = 0.1$, $B_1 = 0.85$, $B_2 = 0.2$, $\omega = 0.45$, $\xi = 0.175$, $V_{\mathrm{syn}} = 2$, $\lambda = 10$, $\theta = -0.25$ [45], the value of τ and d are changed in the case of no-autapse, negative gain autapse (excitatory physiological action) and positive gain autapse (inhibitory physiological action) respectively, and the effects of time delay and coupling strength on dynamics of photosensitive neural networks under different conditions are discussed. The step and time are taken as 0.01 and 2000, respectively, that is we solve the equation set by iterating 200,000 times, the initial value are given as

$$\begin{cases} x_i \mid_{t=0} = 2\cos(2\pi * RandNum) \\ y_i \mid_{t=0} = 2\sin(2\pi * RandNum) \end{cases} \tag{9}$$

and coupling numbers are given as $p = r = 15$, that is each neuron in the network is electrically synaptically coupled to the 15 nearest neurons and chemically coupled to the 15 more distant neurons.

3.1. The Neural Network without Autapse (g = 0)

Let $\tau = 0.8$, the phenomena of asynchronous states, Chimera state and synchronous state can be observed successively in the network by changing the coupling intensity. Figure 2 shows the spatio-temporal diagram of neural network and the phase diagram of membrane potential corresponding to the three states ($t = 1950$). The membrane potential of the neurons in the network is different at the same time when $d = 0.002$, and the asynchronous state is presented as been found in Figure 2a,d. The asynchronous state indicates that the coupling strength is not strong enough to overcome the individual differences among neurons, and each unit of the network maintains its independent discharge rhythm. During brain activities, when visual stimuli are presented, the asynchronous state enables the neural network to maintain a high ability to distinguish different input features, providing the original resolution information for subsequent selective integration. When the coupling intensity is increased to 0.015, it can be observed from Figure 2b,e that some adjacent neurons in the network is synchronous, such as the 82–94 neurons. The synchronous cluster is separated from the non-synchronous cluster, thus a Chimera state is formed. The appearance of the Chimera state indicates that the coupling strength is sufficient to enable some neurons to overcome individual differences and form synchronous clusters, but it is not yet strong enough to unify the entire network. The appearance of a Chimera state in the photosensitive neuron network indicates that the light input did not trigger a globally consistent response but selectively activated some neurons. The synchronous clusters can be understood as clusters of neurons locked by light, the asynchronous clusters, on the other hand, maintain their independent sensitivity to changes in light intensity and continue to monitor other potential light signals in the environment. When $d = 0.03$, the network is stable and synchronized under strong coupling, the membrane potential of 100 neurons is the same as can be found in Figure 2c,f. The emergence of the synchronous state indicates that the coupling strength exceeds the frequency and phase differences caused by the nonlinear oscillations of individual neurons. Synchronization is the foundation of cognitive activities such as movement and perception in the neural system. When the photosensitive neuron network is in a strongly coupling strength, it enters a synchronous state, indicating that the light input can trigger a consistent collective response at the network level, which is conducive to signal integration and downstream transmission.

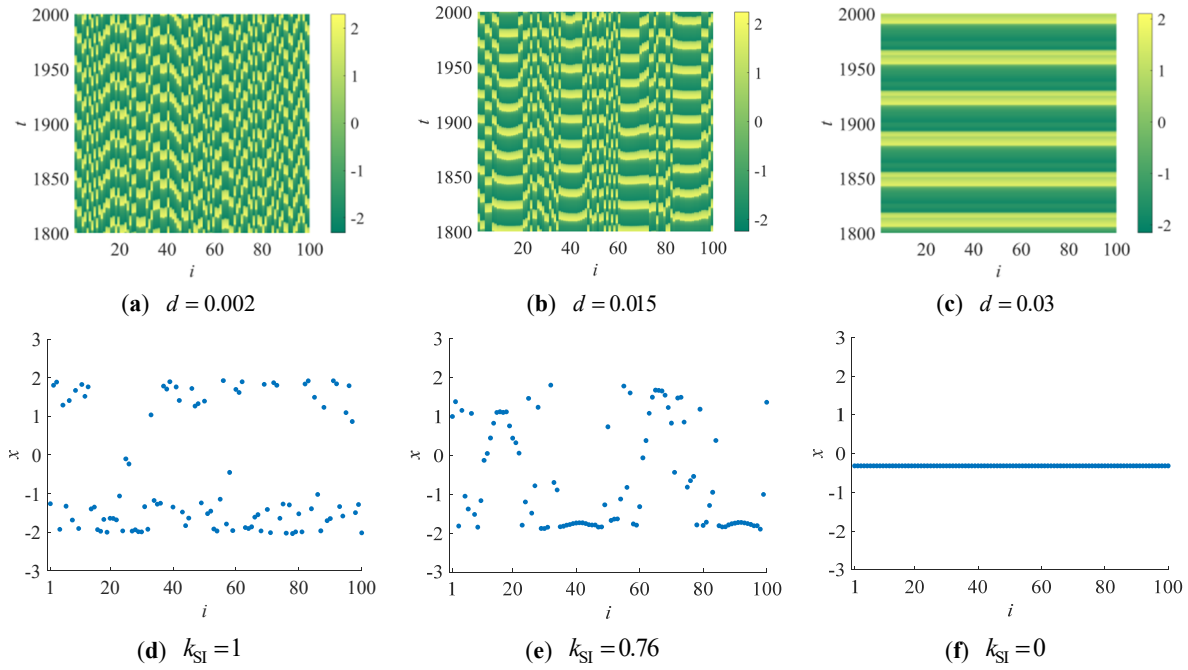


Figure 2. The spatiotemporal patterns and membrane potentials with different coupling strengths for $\tau = 0.8$.

Fixing coupling strength $d = 0.015$, the collective dynamics of the network are observed by changing the delay size. The dynamic phenomena of neural networks are shown in Figure 3b,e when $\tau = 1.5$. The shorter delay causes the coupled signals to accumulate phase in space, and neurons at different locations are activated successively, forming a traveling wave. The value of delay is continuously increased as $\tau = 3$, and the network is in stable synchronization state within the range of $1800 < t < 2000$, as shown in Figure 3c,f. Compared with Figure 2c,f, under the influence of longer time delay, the network tends to reach the synchronous state and no longer relies on strong coupling between neurons. Therefore, in addition to coupling strength, time delay is also a key factor affecting the collective dynamics of neural networks. Appropriate adjustment of the time delay can bring the network as close as possible to its ideal state.

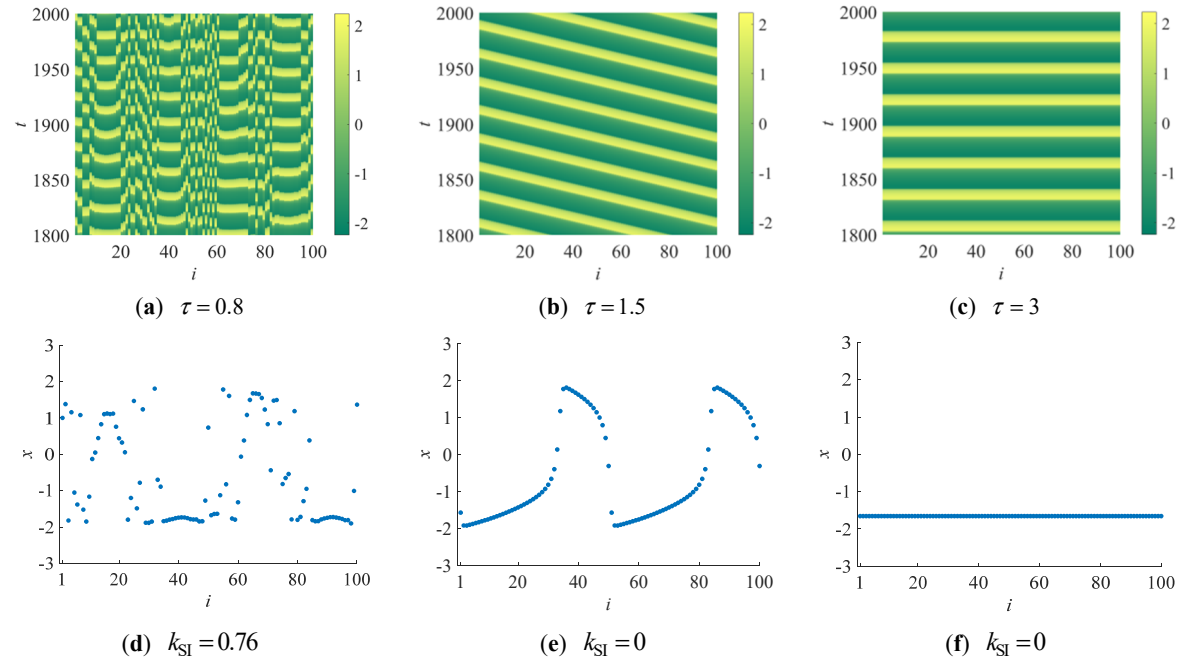


Figure 3. The spatiotemporal patterns and membrane potentials with different time delays for $d = 0.015$.

In order to more intuitively observe the effects of coupling strength and delay on neural networks, $\tau \in [0.5,3]$ and $d \in [0.005,0.03]$ are taken and the two-parameter bifurcation graph of global order parameter k_{SI} is given in Figure 4. The dark blue area corresponds to a synchronized state of the network, indicating a high degree of consistency among the neurons. In contrast, the dark red area indicates that the network is in an asynchronous state, where the membrane potentials of individual neurons exhibit a large degree of dispersion. From Figure 4, the network is the same state when $\tau > 2.1$ and $d \in [0.005,0.03]$, the asynchronous states is stable under the weak coupling condition and $1.5 < \tau < 1.8$, and the Chimera state appears under the condition of small time delay.

Based on Figure 4, we select four coupling strength and draw the tendency graph of k_{SI} and k_{DM} under fixed coupling strength, as shown in Figure 5 and the red dotted line represents the single Chimera state in line chart of k_{DM}. When $d = 0.005, 0.013, 0.021, 0.03$, it is obvious that all the neural networks show a Chimera state under small delay, and synchronization phenomenon exists in the range of $\tau > 2.1$.

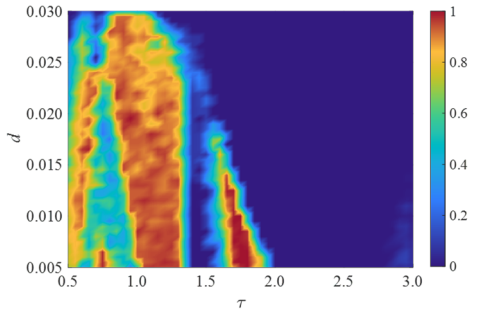


Figure 4. The two-parameter bifurcation graph of parameter plane (τ, d) when $g = 0$.

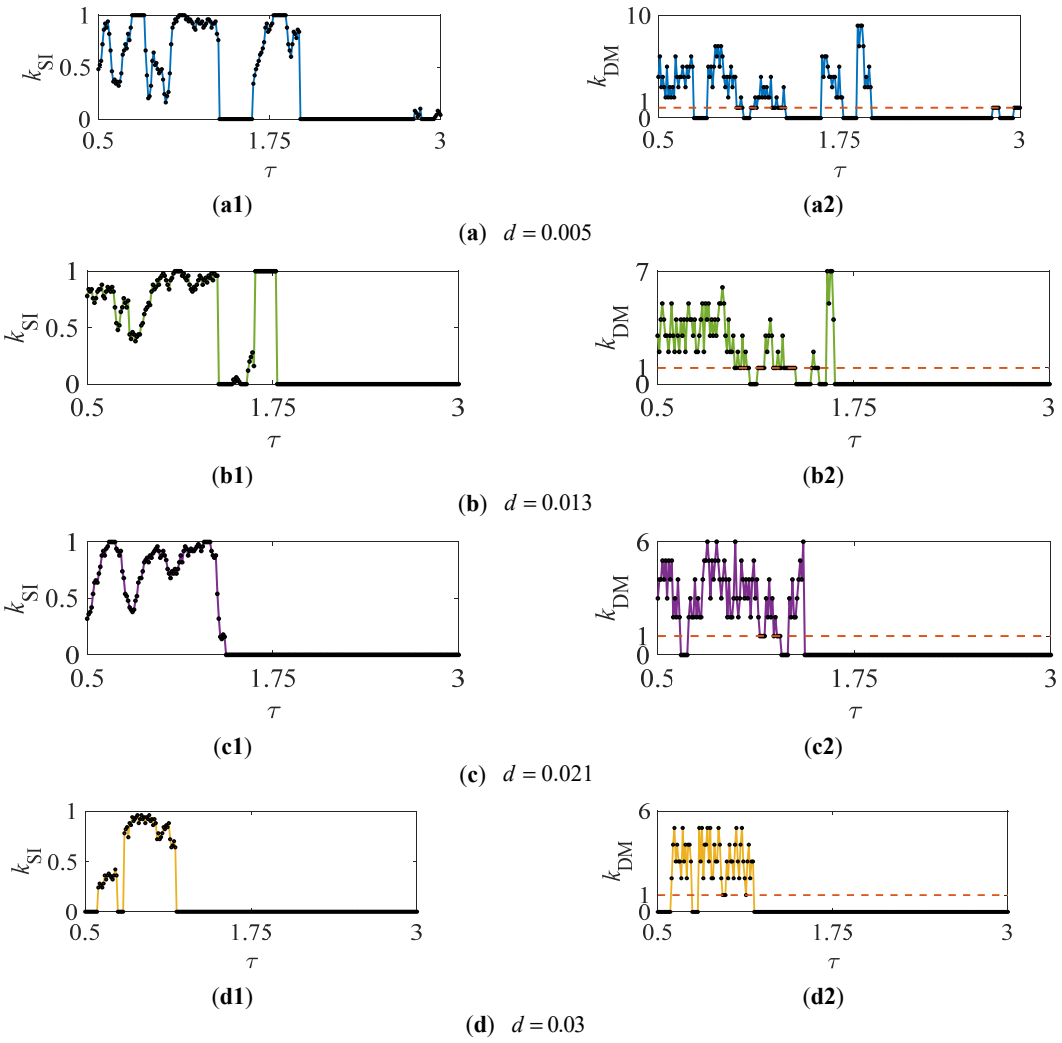


Figure 5. When $g = 0$, the graph of changing trend of k_{SI} and k_{DM} varying time delay.

3.2. The Neural Network with Autapse ($g \neq 0$)

The gain of autapse can affect the collective dynamics of neural networks, so the connection types of positive gain and negative gain are constructed under $g = 0.2$ and $g = -0.2$, then used to investigate the neural networks containing autapse.

When neurons are connected by positive gain of $g = 0.2$ from synapses, Figure 6a,b present the spatiotemporal patterns under the condition of $\tau = 0.8$ and $\tau = 1.5$. From Figure 6a, the neurons number in the synchronization region increases comparing to Figure 3a. In addition, the neural network changes from traveling wave state to homologous states, as can be found in Figure 6b. When the neurons in the network have negative gains of $g = -0.2$ from synaptic connections, Figure 6c,d show the spatiotemporal patterns under the condition of $\tau = 1.5$ and $\tau = 3$. From Figure 6c, we can observe that multiple homologous and non-homologous states appear alternately in the network. Increasing the delay to $\tau = 3$, the network is still in a Chimera state, while the network is in the synchronous states (Figure 3c) without autapse connections. It is further proved that negative gain synapses cause the neural network to tend towards an asynchronous state, while under the influence of positive gain, the neural network tends towards a synchronous state.

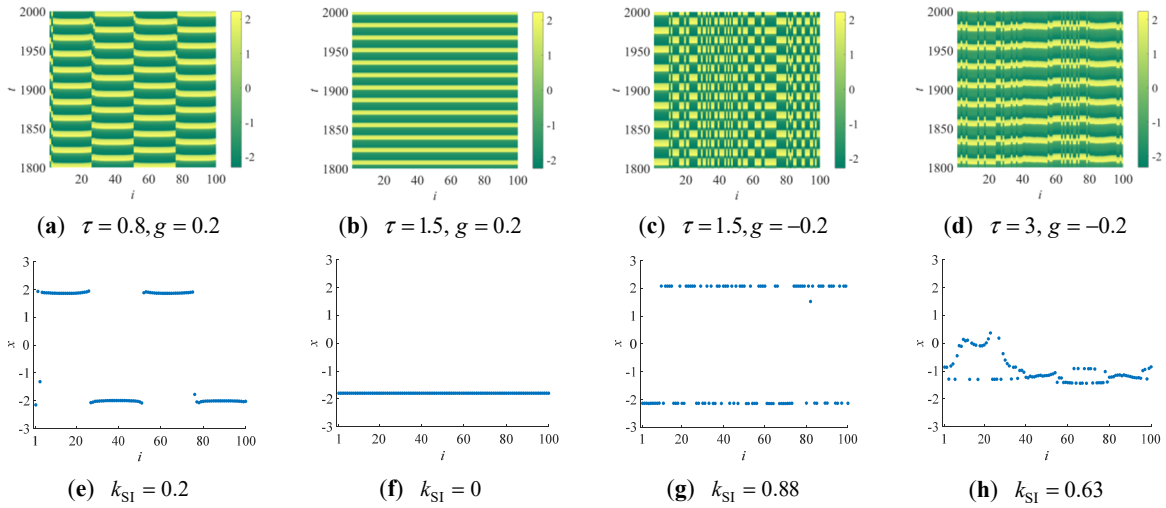


Figure 6. The spatiotemporal patterns and snapshots of the network with different time delays and autapse gains for $d = 0.015$.

3.2.1. The Neural Network with Autapse ($g = -0.2$)

Figure 7 shows the two-parameter bifurcation of k_{SI} under plane (d, τ), it is found that when $d \in [0.005, 0.03]$, the Chimera states are more distributed under the condition of very small or very large delay. When $d = 0.005, 0.013, 0.021, 0.03$ respectively, the graph of changing trend of k_{SI} and k_{DM} is given in Figure 8. We focus $1.3 < \tau < 1.9$, k_{SI} is close to 0 and the network always approaches synchronization or is in a synchronous state (Figure 8a,b), whereas k_{SI} identically equals to 0 and the network presents synchronous states (Figure 8c,d). It can be obtained from the trend graph of k_{DM} that most of the Chimera states in this network exist in the form of multiple cluster Chimera states.

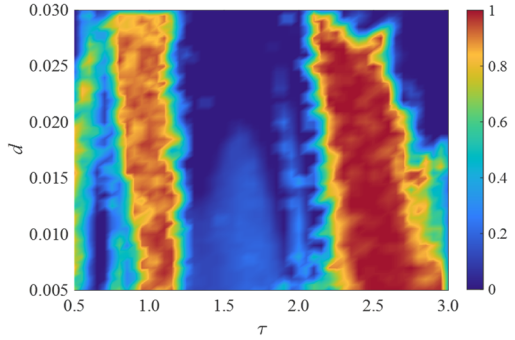


Figure 7. The two-parameter bifurcation graph of parameter plane (τ, d) when $g = -0.2$.

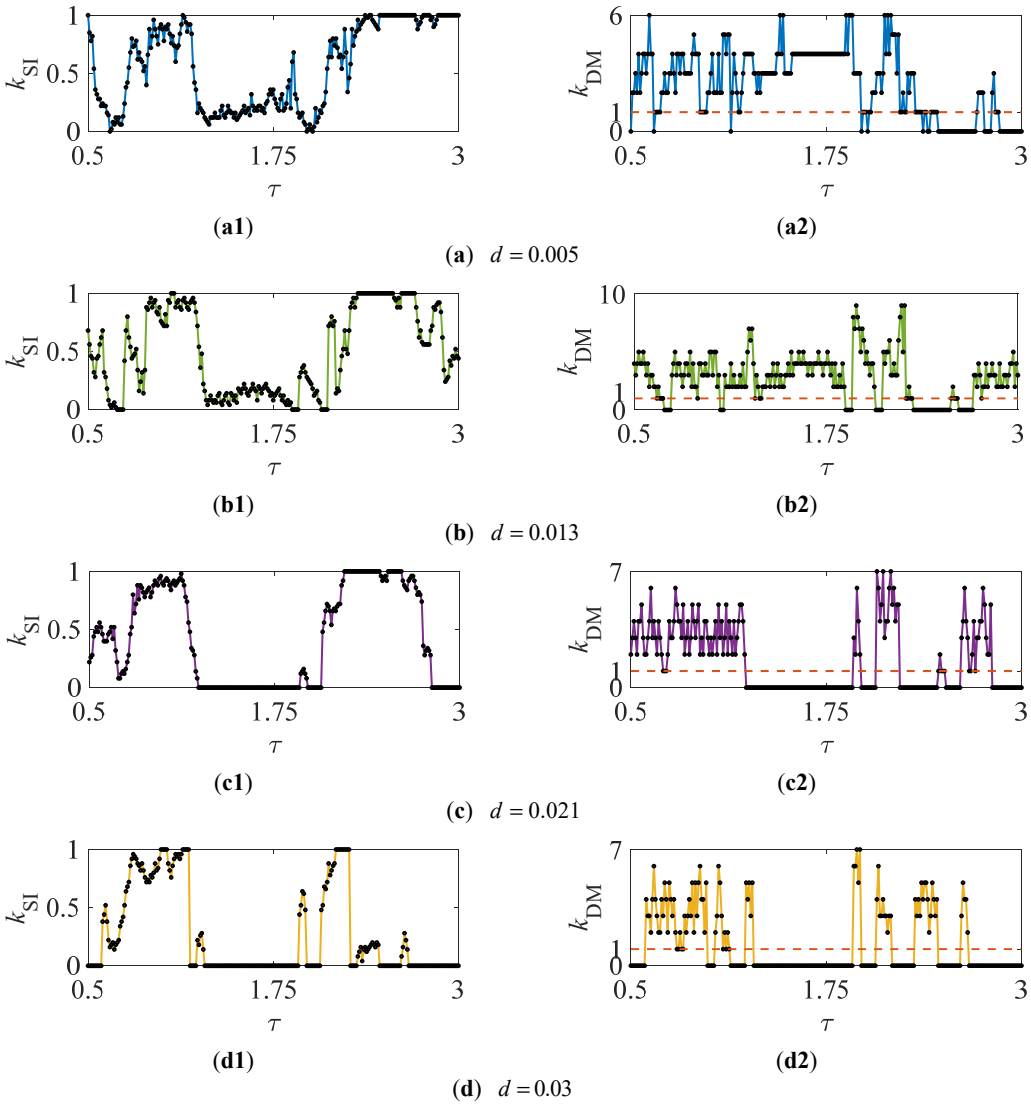


Figure 8. When $g = -0.2$, the graph of changing trend of k_{SI} and k_{DM} varying time delay.

3.2.2. The Neural Network with Autapse ($g = 0.2$)

Under positive gain occurs from synaptic connection, two-parameter bifurcation diagram of plane (d, τ) is presented in Figure 9. Neurons only exhibit Chimera states and asynchronous states in a small area of $\tau \in [0.5, 3], d \in [0.005, 0.03]$ as shown in Figure 9b. It is similar to the changing trend in Figure 4, the Chimera states in the network exist under small time delay, while the network with a longer time delay always maintains synchronous states. It can be seen from Figure 10 that the Chimera state categories in this network are mainly multi-cluster Chimera states.

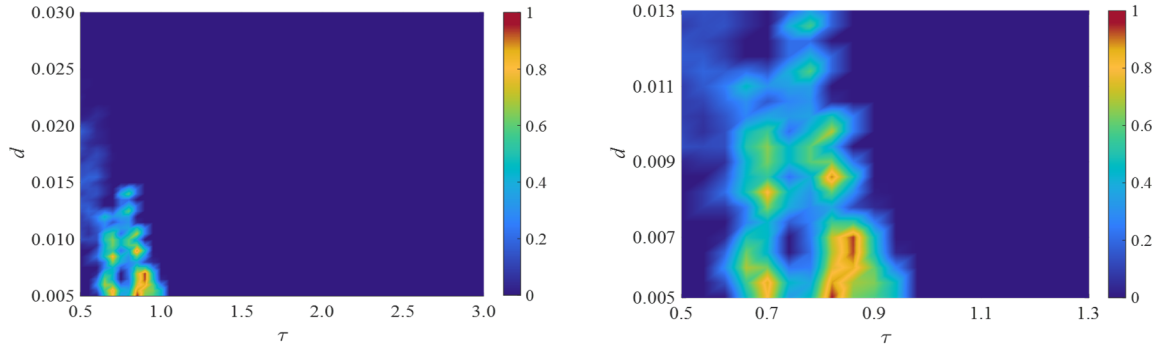


Figure 9. The two-parameter bifurcation graph of parameter plane (τ, d) when $g = 0.2$.

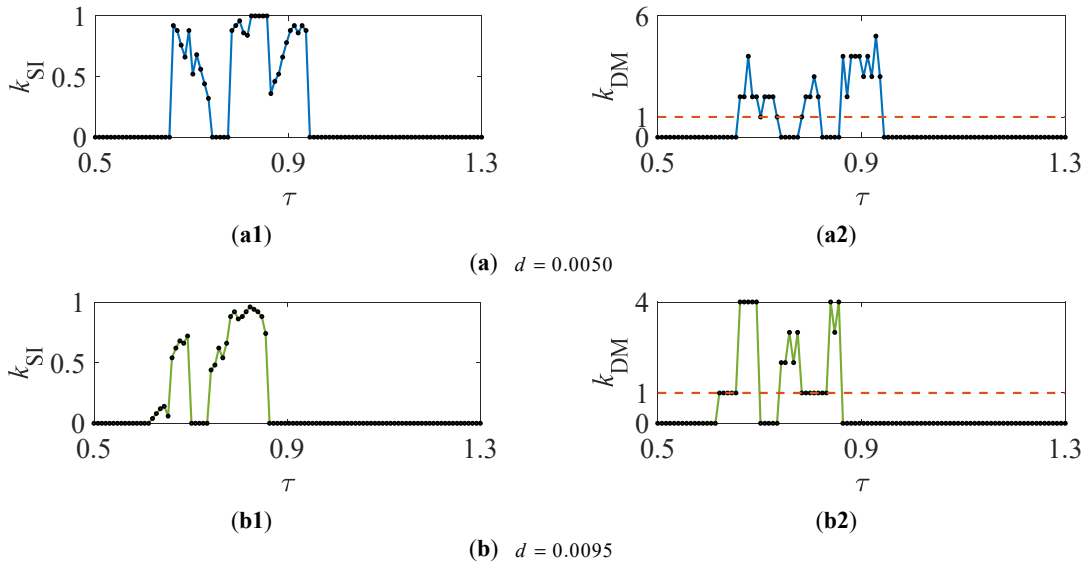


Figure 10. When $g = 0.2$, the graph of changing trend of k_{SI} and k_{DM} varying time delay.

Yilmaz et al. [46] showed that autaptic time delay can induce multiple coherence resonance at both the single-neuron and network levels, and that the coherence resonance and synchronization transition at the network level occur at nearly the same delay length, although these phenomena appear only within a specific range of coupling strength. When the delay is shorter than the refractory period, the autapse reduces firing regularity; when the delay exceeds the refractory period, firing regularity can be significantly enhanced by appropriately adjusting the autaptic conductance. A comparison between Figures 7 and 9 shows that, in the photosensitive neuronal network, a positive-gain autapse (negative feedback) drives the network toward synchronization, whereas a negative-gain autapse (positive feedback) drives it toward asynchrony. This indicates that the regulation of network dynamics by autapses depends not only on the autaptic time delay, but also on the feedback type, which is likewise a key parameter determining the collective state.

4. Conclusions

Based on the single-layer photosensitive neural network with nonlocal coupling, the coupling scheme is changed from a single electrical synaptic coupling to a mixed coupling scheme involving both electrical and chemical synapses. For neural networks without autapses and with autapses, the coupling strength and time delay are varied to investigate their effects on the dynamic behavior of the neural networks. From the research, it is found that the photosensitive neural network not only changes its state due to different coupling strengths and time delays, but also the autapse can affect the synchronous state, Chimera state and asynchronous state within the network. In the neural network without autapse, a long time delay will promote the neurons in the network to tend to the same discharge frequency, thereby achieving stable synchronization. Conversely, in the neural network with negative-gain autapses, asynchronous phenomena occur under the influence of long time delays, whereas shorter time delays can better stabilize the Chimera state in the network. In the neural network with positive-gain autapses, the range of states affected by time delay is significantly reduced, and more precise parameter values are required to accurately induce Chimera and asynchronous states in the neural network. Compared with the single Chimera state, the frequency of multiple clustered Chimera states occurring in the network is higher. This provides theoretical support for understanding how the real visual system regulates information processing patterns through the coupling strength, time delay and feedback between synapses, and also offers parameter references for the design of neuromorphic optoelectronic computing devices.

Author Contributions

X.A.: wrote the main manuscript text and prepared figures and tables; X.W.: carried out preliminary investigations, planning and overall coordination of the entire process. Both authors have read and agreed to the published version of the manuscript.

Funding

This work is supported from the National Natural Science Foundation (No. 62541121), the Gansu Key Research and Development Program (No. 24YFGA040), the Gansu Province Natural Science Foundation of China (No. 24JRRA291).

Institutional Review Board Statement

Not applicable.

Informed Consent Statement

Not applicable.

Data Availability Statement

Data will be made available on reasonable request.

Conflicts of Interest

The authors declare no conflict of interest.

Use of AI and AI-Assisted Technologies

No AI tools were utilized for this paper.

References

1. Balood, M.; Ahmadi, M.; Eichwald, T.; et al. Nociceptor neurons affect cancer immunosurveillance. *Nature* **2022**, *611*, 405–412. https://doi.org/10.1038/s41586-022-05374-w.
2. Cavanaugh, J.; Mcalonan, K.; Wurtz, R.H. Organization of corollary discharge neurons in monkey medial dorsal thalamus. *J. Neurosci.* **2020**, *40*, 6367–6378. https://doi.org/10.1523/JNEUROSCI.2344-19.2020.
3. Ji, Y.S.; Mao, X.C. Stochasticity-induced enhanced synchronization in memristive FitzHugh-Nagumo systems: A numerical investigation. *Nonlinear Dynam.* **2026**, *114*, 291. https://doi.org/10.1007/s11071-025-12171-3.
4. Ma, J. Biophysical neurons, energy, and synapse controllability: A review. *J. Zhejiang Univ.-Sci. A* **2023**, *24*, 109–129. https://doi.org/10.1631/jzus.a2200469. (In Chinese)
5. Chauhan, K.; Neiman, A.B.; Tass, P.A. Synaptic reorganization of synchronized neuronal networks with synaptic weight and structural plasticity. *PLoS Comput. Biol.* **2024**, *20*, e1012261. https://doi.org/10.1371/journal.pcbi.1012261.
6. Jiang, L.; Xiong, L.; An, X.; et al. Phase synchronization under mixed synapse between two heterogeneous functional neurons. *Phys. Scr.* **2023**, *98*, 115243. https://doi.org/10.1088/1402-4896/ad00e4.
7. Li, Z.; Klein, J.A.; Rampam, S.; et al. Asynchronous excitatory neuron development in an isogenic cortical spheroid model of Down syndrome. *Front. Neurosci.* **2022**, *16*, 932384. https://doi.org/10.3389/fnins.2022.932384.
8. Glaze, T.A.; Bahar, S. Neural Synchronization, Chimera States and Sleep Asymmetry. *Front. Netw. Physiol.* **2021**, *1*, 734332. https://doi.org/10.3389/fnetp.2021.734332.
9. Jacimovic, V.; Crnkic, A. Möbius group actions in the solvable chimera model. *Int. J. Mod. Phys. B* **2025**, *39*, 2540005. https://doi.org/10.1142/s0217979225400053.
10. Márquez-Rodríguez, V.J.; Tucci, K.; Cosenza, M.G. Chimera states and information transfer in interacting populations of map-based neurons. *Neural Comput. Appl.* **2024**, *36*, 18151–18159. https://doi.org/10.1007/s00521-024-10050-3.
11. Muni, S.S.; Njitacke, Z.T.; Feudjio, C.; et al. Route to Chaos and Chimera States in a Network of Memristive Hindmarsh-Rose Neurons Model with External Excitation. *Chaos Theory Appl.* **2022**, *4*, 119–127. https://doi.org/10.51537/chaos.1144123.
12. Yuan, Y.; Yang, H.; Han, F.; et al. Traveling chimera states in locally coupled memristive Hindmarsh-Rose neuronal networks and circuit simulation. *Sci. China Technol. Sci.* **2022**, *65*, 1445–1455. https://doi.org/10.1007/s11431-021-2042-4.
13. Rybalova, E.; Schöll, E.; Strelkova, G. Controlling chimera and solitary states by additive noise in networks of chaotic maps. *J. Differ. Equ. Appl.* **2023**, *29*, 909–930. https://doi.org/10.1080/10236198.2022.2118580.
14. Remi, T.; Subha, P.A. Emergence of chimera states in neural networks with distance-dependent mean field coupling. *Int. J. Mod. Phys. C* **2024**, *35*, 2450107. https://doi.org/10.1142/s0129183124501079.
15. Andrzejak, R.G.; Espinoso, A. Chimera states in multiplex networks: Chameleon-like across-layer synchronization. *Chaos Interdiscip. J. Nonlinear Sci.* **2023**, *33*, 053112. https://doi.org/10.1063/5.0146550.

16. Xi, X.; Yang, R.; Zhang, P.; et al. Synchronization in a neuronal network with delayed hybrid synapses. *Eur. Phys. J. Spec. Top.* **2025**, *234*, 979–989. https://doi.org/10.1140/epjs/s11734-025-01671-3.
17. Azangue, A.B.; Ngouonkadi, E.B.M.; Nono, M.K.; et al. Collective Behavior in Neuronal Networks with Electrical and Hybrid Synapses: Frequency Responses of Oscillations. *Int. J. Bifurc. Chaos* **2023**, *33*, 2330005. https://doi.org/10.1142/s0218127423300057.
18. Goel, M.; Mangel, S.C. Dopamine-mediated circadian and Light/Dark-Adaptive modulation of chemical and electrical synapses in the outer retina. *Front. Cell. Neurosci.* **2021**, *15*, 647541. https://doi.org/10.3389/fncel.2021.647541.
19. Liu, H.; Shen, Y.; Zhao, Y. Spiking Neural P Systems with Anti-Spikes and Autapses. *Int. J. Unconv. Comput.* **2026**, *21*, 129–142. https://doi.org/10.32908/ijuc.v21.zhang05.
20. Vijayan, V.; Vo, T.P. Delay-induced synchronization in a multiplex neuronal network. *Eur. Phys. J. Spec. Top.* **2025**, *234*, 963–977. https://doi.org/10.1140/epjs/s11734-025-01670-4.
21. Shavikloo, M.; Esmaeili, A.; Valizadeh, A.; et al. Synchronization of delayed coupled neurons with multiple synaptic connections. *Cogn. Neurodyn.* **2024**, *18*, 631–643. https://doi.org/10.1007/s11571-023-10013-9.
22. Zou, L.; Wang, S.; Zhang, H.; et al. Delay learning for spiking neurons with multiple synaptic connections. *Proc. Rom. Acad. Ser. A* **2025**, *26*, 89–99. https://doi.org/10.59277/pra-ser.a.26.1.11.
23. Huang, S.; Yu, C.; Cai, Z.; et al. Frequency chimera state induced by time delays in FitzHugh-Nagumo neural networks. *Chin. J. Phys.* **2024**, *92*, 115–123. https://doi.org/10.1016/j.cjph.2024.09.009.
24. Hou, J.; Liu, Q.; Yang, H.; et al. Stability and bifurcation analyses of p53 gene regulatory network with time delay. *Electron. Res. Arch.* **2022**, *30*, 850–873. https://doi.org/10.3934/era.2022045.
25. Dong, S.; Zhu, H.; Zhong, S.; et al. New study on fixed-time synchronization control of delayed inertial memristive neural networks. *Appl. Math. Comput.* **2021**, *399*, 126035. https://doi.org/10.1016/j.amc.2021.126035.
26. Ma, J. Dynamics and model approach for functional neurons. *J. Guangxi Norm. Univ. (Natl. Sci. Ed.)* **2022**, *40*, 307–323. (In Chinese)
27. An, X.; Jiang, L.; Xiong, L.; et al. Synchronization behavior and energy evolution in physical neuron and network. *Nonlinear Dyn.* **2024**, *112*, 16389–16407. https://doi.org/10.1007/s11071-024-09882-4.
28. Yang, F.; Zhou, P.; Ma, J. An adaptive energy regulation in a memristive map linearized from a circuit with two memristive channels. *Commun. Theor. Phys.* **2024**, *76*, 035004. https://doi.org/10.1088/1572-9494/ad260e.
29. Zhang, L.; An, X.; Zhang, J. Field coupling-induced synchronization of a functional neuron with magnetic field perception. *Phys. Scr.* **2023**, *98*, 045203. https://doi.org/10.1088/1402-4896/acbdc6.
30. Zhou, P.; Yao, Z.; Ma, J.; et al. A piezoelectric sensing neuron and resonance synchronization between auditory neurons under stimulus. *Chaos Solitons Fractals* **2021**, *145*, 110751. https://doi.org/10.1016/j.chaos.2021.110751.
31. Zhou, S.; Cheng, Z.; Huang, G.; et al. Synchronization evaluation of memristive photosensitive neurons in multi-neuronal systems. *Chaos Solitons Fractals* **2024**, *187*, 115470. https://doi.org/10.1016/j.chaos.2024.115470.
32. Ji, Y.; Mao, X. Complex firing patterns of a delayed thermosensitive neuronal network with synaptic crosstalk. *Nonlinear Dyn.* **2026**, *114*, 381. https://doi.org/10.1007/s11071-026-12265-6.
33. Chen, K.; Li, Z. Astrocyte mediated firing activities and synchronization in a heterogeneous neuronal network. *Chaos Solitons Fractals* **2024**, *188*, 115564. https://doi.org/10.1016/j.chaos.2024.115564.
34. Vivekanandhan, G.; Mehrabbeik, M.; Natiq, H.; et al. Synchronization and firing patterns of coupled one-dimensional neuron maps. *Pramana* **2023**, *97*, 171. https://doi.org/10.1007/s12043-023-02628-8.
35. Fan, W.; Chen, X.; Wu, H.; et al. Firing patterns and synchronization of Morris-Lecar neuron model with memristive autapse. *AEU-Int. J. Electron. Commun.* **2023**, *158*, 154454. https://doi.org/10.1016/j.aeue.2022.154454.
36. Yang, F.; Ma, J. Synchronization and energy balance of star network composed of photosensitive neurons. *Eur. Phys. J. Spec. Top.* **2022**, *231*, 4025–4035. https://doi.org/10.1140/epjs/s11734-022-00698-0.
37. Han, W.; Qin, Z.; Liu, J.; et al. Synchronization-Inspired Interpretable Neural Networks. *IEEE Trans. Neural Netw. Learn. Syst.* **2024**, *35*, 16762–16774. https://doi.org/10.1109/tnnls.2023.3297672.
38. Huang, W.; Wu, Y.; Ding, Q.; et al. Achieving synchronization and chimera state of modular neural networks by using dynamic learning to adjust electromagnetic induction. *Nonlinear Dyn.* **2025**, *113*, 6671–6693. https://doi.org/10.1007/s11071-024-10435-y.
39. Rybalova, E.; Semenova, N. Impact of pulse exposure on chimera state in ensemble of FitzHugh–Nagumo systems. *Chaos Interdiscip. J. Nonlinear Sci.* **2024**, *34*, 071101. https://doi.org/10.1063/5.0214787.
40. Stroh, A.; Schweiger, S.; Ramirez, J.M.; et al. The selfish network: How the brain preserves behavioral function through shifts in neuronal network state. *Trends Neurosci.* **2024**, *47*, 246–258. https://doi.org/10.1016/j.tins.2024.02.005.
41. Ragavan, A.; Manoranjani, M.; Senthilkumar, D.V.; et al. Multistable chimera states in a smallest population of three coupled oscillators. *Phys. Rev. E* **2023**, *107*, 044209. https://doi.org/10.1103/physreve.107.044209.
42. Li, H.; Xie, Y. Alternating chimera states and synchronization in multilayer neuronal networks with ephaptic intralayer coupling. *Cogn. Neurodyn.* **2024**, *18*, 3847–3858. https://doi.org/10.1007/s11571-024-10169-y.

43. Feng, P.; Yang, J.; Wu, Y.; et al. Alternating chimera states in complex networks with modular structures. *Chaos Interdiscip. J. Nonlinear Sci.* **2023**, *33*, 033136. https://doi.org/10.1063/5.0132072.
44. Gopal, R.; Chandrasekar, V.K.; Venkatesan, A.; et al. Observation and characterization of chimera states in coupled dynamical systems with nonlocal coupling. *Phys. Rev. E* **2014**, *89*, 052914. https://doi.org/10.1103/physreve.89.052914.
45. Xie, Y.; Zhu, Z.G.; Zhang, X.F.; et al. Control of discharge patterns in nonlinear neuron circuits driven by photocurrent. *Chin. J. Phys.* **2021**, *70*, 106–116.
46. Yilmaz, E.; Ozer, M.; Baysal, V.; et al. Autapse-induced multiple coherence resonance in single neurons and neuronal networks. *Sci. Rep.* **2016**, *6*, 30914. https://doi.org/10.1038/srep30914.